Journal of Biomechanics 33 (2000) 1695–1699

JOURNAL OF BIOMECHANICS

www.elsevier.com/locate/jbiomech

Technical note

Comparison of different calculations of three-dimensional joint kinematics from video-based system data

Laurence Chèze

Laboratoire de Mécanique de l'Appareil Locomoteur Bât. 721, Université Claude Bernard (Lyon 1), 43 Bd. du 11 novembre 1918, 69622 Villeurbanne Cedex, France

Accepted 23 June 2000

Abstract

When skin-fixed marker trajectories are used to calculate 3D joint kinematics, the measurement errors (i.e. the difference between the trajectories of the external markers and those of the skeleton) influence to some extent the accuracy of the results, depending both on the calculation method and on the axes about which the rotations are expressed. The purpose of this paper is to compare several expressions of joint angular variations. Two kinematic concepts are used to calculate the changes in the orientation of the distal segment versus the proximal one: the first method consists of computing the components of the spatial attitude vector, the second one deals with the determination of elementary rotations about successive axes. For each of these methods, two sets of three axes are tested to express the results: the axes forming the reference frame affixed to the body segment adjacent to the joint (named *fixed axes*), and a set consisting of a first axis belonging to the proximal segment, a third axis belonging to the distal segment and a second (floating) axis defined as the cross-product between the two other ones (named *mobile axes*). To compare these four distinct expressions on the knee joint, numerical simulations of perturbed skin marker trajectories are performed, based on experimental data recorded by a Motion Analysis system during a normal gait cycle. A significant difference is pointed out only for the internal–external rotation angle, for which the best expression — from the viewpoint of sensitivity to experimental errors — is obtained using the components of the attitude vector in a segment-embedded reference frame.

Keywords: Spatial attitude vector; Sequence of elementary rotations; Influence of measurement noise; Kinematics standardisation

1. Introduction

Video-based motion analysis systems are often used to estimate segmental kinematics. A common assumption consists of modelling the human limbs as rigid segments, linked together by more or less complex joints. It is then legitimate to apply rigid-body kinematics on this mechanical system.

Nevertheless, the trajectories measured by motion analysis systems are those of individual markers, glued on the subject skin. All measurement systems generate high frequency noise on the trajectories, which can be easily decreased using an adapted low-pass filter (Mann and Antonsson, 1983; Fioretti and Jetto, 1989), but other kinds of perturbations are more difficult to eliminate. Many studies have shown that important relative displacements exist between skin-fixed markers and corresponding anatomical landmarks (Andriacchi, 1987; Lafortune et al., 1992; Cappello et al., 1997; Lucchetti et al., 1998). Some authors have given partial solutions to this problem, using numerical algorithms based on least-squares methods (Veldpaus et al., 1988; Söderkvist and Wedin, 1993; Chèze et al., 1995a) or on filtering techniques with distance constraints (Chèze and Fioretti, 1995b). However, these methods are only effective on the uncorrelated part of the individual marker displacement with respect to the underlying bone.

It follows that the selection, among the numerous methods known in the mechanical field to describe rigid-body motions, of the one more likely to give accurate results from skin marker trajectories is of great interest.

Many studies use sequences of elementary rotations to describe joint kinematics (Spoor and Veldpaus, 1980; Chao, 1980; Grood and Suntay, 1983); others make use of helical axes (or spatial attitude vectors) (Woltring et al., 1983; Dimnet and Guingand, 1984; Spoor, 1984; Woltring et al., 1985; Blankevoort et al., 1990). The interest in the concept of helical axis is the uniqueness of the description (Woltring, 1994), whereas the rotation

0021-9290/00/$ - see front matter
PII: S0021-9290(00)00146-9

amplitudes calculated using a sequence obviously depend on the sequence order (Skalli et al., 1995). However, the helical axis characteristics, classically used to follow the relative displacement between two adjacent body segments, are very sensitive to noise (Chèze et al., 1998). Furthermore, the relative rotation so described (i.e., the relative orientation of the distal segment, the proximal one being assumed motionless) does not correspond to that obtained using a sequence of elementary rotations.

Another use of the spatial attitude vector is proposed in this paper to express joint kinematics. It consists of computing directly, at each instant of time, the components of the spatial vector characterising the distal segment orientation with respect to the proximal one (Chèze, 1998). The joint evolutions so calculated are compared with those obtained using a sequence of elementary rotations. This comparison deals mainly with the sensitivity of the results to marker trajectory perturbations.

2. Materials and methods

To follow the joint kinematics during a given movement, the spatial attitude vector $\boldsymbol{k}\theta$ and a sequence of elementary rotations are computed. For both descriptions, the neutral position (i.e., nil rotation values on all axes) corresponds to the situation where the reference frames embedded in the adjacent segments are aligned. In the case of successive rotations, the angles are computed either about fixed axes or about mobile axes. For comparison purposes, the attitude vector $\boldsymbol{k}\theta$ is projected onto the same fixed and mobile axes. A numerical simulation is used to test the sensitivity of the results obtained from these different expressions to the same measurement noise. This simulation is based on experimental data, which makes it possible to verify the consistency of the results with clinical interpretations.

The experimental trajectories are those of ten markers glued on the lower limb segments. Four skin markers define the pelvis (left and right anterior/posterior iliac spines), three markers define the thigh (greater trochanter, medial and lateral epicondyles of the femur) and three markers are glued on the shank (tibial tuberosity, internal and external malleoli). These trajectories are measured using a video-based motion analysis system (Motion Analysis Corp., Santa Rosa, CA), equipped with six cameras. The subject (a 25 year-old man) is walking at normal speed and the motion of the right limb is recorded during one gait cycle, at a frequency of 60 frames per s. The 3D trajectories of the markers are then filtered using a Butterworth digital filter (cut-off frequency = 5 Hz) to eliminate the high frequency noise due to the measurement system, and "solidified" using the algorithm described in Chèze et al. (1995a) to obtain trajectories consistent with a rigid-body assumption. To these reference data, a random noise representing mainly the measurement errors due to the perturbating displacement of skin-fixed markers with respect to anatomical landmarks is added. A noise model of the form $\Delta x_{i,j} = A_{i,j}\sin(\omega_{i,j}t + \phi_{i,j})$ (for co-ordinate $i = 1$–3 and marker $j = 1$–10) is chosen (Chèze et al., 1998). The amplitude A, the pulsation ω and the phase angle ϕ are selected at random in the ranges $0 \leqslant A \leqslant 1$ cm, $0 \leqslant \omega \leqslant 6 - \mathrm{rad} - \mathrm{s}^{-1}, 0 \leqslant \phi \leqslant 2\pi$, which correspond to perturbations observed experimentally (Andriacchi, 1987; Cappello et al., 1997). Each marker co-ordinate is then calculated at each instant of time by the relation: $x_{i,j} = (x_{i,j})_{\mathrm{ref}} + \Delta x_{i,j}$.

On both reference and noisy trajectories, the rotation operator $\mathbf{R}_{T,S}$ describing the change of orientation from the thigh reference frame to the shank one is computed at each instant of time. For this, a reference frame is defined on each body segment. The conventions proposed in the European CAMARC II project (Cappozzo et al., 1995) have been retained for the thigh: the $\boldsymbol{Y}_\mathrm{T}$ axis joins the midpoint between the markers glued on the femoral condyles (chosen as the origin $\mathrm{O_T}$) and the hip centre H calculated by the procedure described in the next paragraph; the $\boldsymbol{X}_\mathrm{T}$ axis is perpendicular to $\boldsymbol{Y}_\mathrm{T}$ and to the direction defined by the two femoral condyles, it points forward; at last, the $\boldsymbol{Z}_\mathrm{T}$ axis is computed as the cross-product of the unit vectors $\boldsymbol{X}_\mathrm{T}$ and $\boldsymbol{Y}_\mathrm{T}$.

The hip joint centre H is determined, using marker trajectories collected during a circumduction motion, as follows. The finite helical axes describing, at each instant of time, the attitude of the thigh with respect to the pelvis are first computed. Then, the joint centre is determined as the convergence point of the bundle of helical axes. Actually, when the anatomical joint can be viewed as a spherical joint (as is the case for the hip joint), the spherical joint centre coincides with the convergence point of the bundle of helical axes.

The reference frame $\mathbf{F}_\mathrm{S}$, affixed to the shank, is chosen superimposed to that of the thigh $\mathbf{F}_\mathrm{T}$ on a static reference position. This assumption is required in order that both the elementary rotations and the components of the spatial attitude vector $\boldsymbol{k}\theta$ be zero for this particular position. This reference frame definition does not affect the results since the attitude vector components are, by definition, identical at each instant of time in both the distal and proximal segment reference frames.

The rotation operator $\mathbf{R}_\mathrm{T,S}$ is computed at each instant of the motion by $\mathbf{R}_\mathrm{T,S} = ({}^0_\mathrm{T}\mathbf{R})^{-1}.\ {}^0_\mathrm{S}\mathbf{R}$, where ${}^0_\mathrm{T}\mathbf{R}$ (respectively ${}^0_\mathrm{S}\mathbf{R}$) is a rotation matrix of which the columns are the components of the thigh reference frame $\mathbf{F}_\mathrm{T}$ axes (respectively $\mathbf{F}_\mathrm{S}$) in the fixed laboratory frame $\mathbf{F}_0$.

When successive rotations are computed, $\mathbf{R}_\mathrm{T,S}$ is given by the product of elementary rotation matrices. As the knee joint is considered, the generally used convention of Grood and Suntay (1983) is chosen to avoid the "gimbal-lock" phenomenon: the first rotation (α) takes place about the flexion axis of the thigh $\boldsymbol{Z}_T$, the last rotation (γ) takes place about the internal–external rotation of the shank $\boldsymbol{Y}_s$, and the abduction–adduction component (β) is about a floating axis defined by the cross-product of $\boldsymbol{Y}_S$ and $\boldsymbol{Z}_T$.

If an expression about the fixed axes (i.e., reference frame $\mathbf{F}_T$ embedded in the proximal segment) is required, the product of these elementary rotation matrices may be performed backwards. In this case, the flexion component (α) still takes place about $\boldsymbol{Z}_T$ but the abduction–adduction (β) and internal–external rotation (γ) are computed, respectively, about the $\boldsymbol{X}_T$ and $\boldsymbol{Y}_T$ axes.

The spatial attitude vector $\boldsymbol{k}\theta$ can also be derived from the rotation operator $\mathbf{R}_{T,S}$ (Woltring et al., 1985). Note that the components are directly obtained in both segment embedded reference frames $\mathbf{F}_T$ and $\mathbf{F}_S$. To compare the expressions relative to the mobile axes, this spatial vector is projected onto the axes $\boldsymbol{X}, \boldsymbol{Y}_S, \boldsymbol{Z}_T$ of the Grood & Suntay's convention. This yields the relation

$$\boldsymbol{k}\theta = \frac{(\boldsymbol{Y}_S, \boldsymbol{Z}_T, \boldsymbol{k}\theta)}{(\boldsymbol{X}, \boldsymbol{Y}_S, \boldsymbol{Z}_T)}\boldsymbol{X} + \frac{(\boldsymbol{Z}_T, \boldsymbol{X}, \boldsymbol{k}\theta)}{(\boldsymbol{X}, \boldsymbol{Y}_S, \boldsymbol{Z}_T)}\boldsymbol{Y}_S + \frac{(\boldsymbol{X}, \boldsymbol{Y}_S, \boldsymbol{k}\theta)}{(\boldsymbol{X}, \boldsymbol{Y}_S, \boldsymbol{Z}_T)}\boldsymbol{Z}_T$$

where $\boldsymbol{X}$ is defined by the cross product $\boldsymbol{X} = \boldsymbol{Y}_S \times \boldsymbol{Z}_T$ and $(\boldsymbol{X}, \boldsymbol{Y}, \boldsymbol{Z})$ refers to the mixed product.

The mean (resp. maximum) errors, as well as the mean and maximum dispersions, have been calculated as the mean (resp. maximum) values on the whole set of images in the gait cycle, of the following expressions:

$$\text{error} = \sum_{i=1}^{n} \frac{|\theta_{\text{ref}} - \theta_{\text{p,i}}|}{n},$$

$$\text{dispersion} = \frac{\sqrt{\sum_{i=1}^{n}(\theta_{\text{ref}} - \theta_{\text{p,i}})^2}}{n},$$

where n is the number of trials ($n = 50$), θ_{ref} and $\theta_{\text{p,i}}$ are, respectively, the reference and perturbed rotation components (for trial No. i), at a given image of the gait cycle.

3. Results

A comparison of two concepts (the spatial rotation vector $\boldsymbol{k}\theta$ and the sequence of elementary rotations) is shown and for each of these concepts two expressions (relative to fixed and mobile axes, respectively) are compared. These different computations are done both on reference data and on numerically perturbed data, corresponding to the 3D trajectories of markers fixed on thigh and shank segments during a gait cycle.

The series of curves (Fig. 1) displays the disparity between the angular values obtained from the four distinct expressions, when reference data are identical. This disparity is illustrated by the ratio between the maximum amplitude difference and the average amplitude for each component. This ratio is 5, 16 and 90% , respectively, on

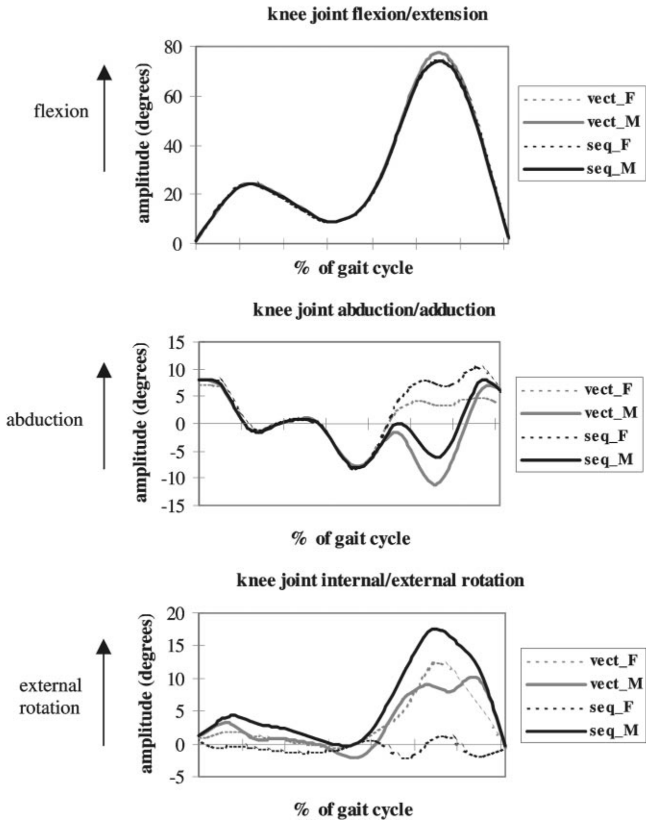

Fig. 1. Time variations of knee joint angles obtained using the four distinct expressions on reference data. **vect_F**: spatial attitude vector $\boldsymbol{k}\theta$ expressed on fixed axes. **vect_M**: spatial attitude vector $\boldsymbol{k}\theta$ expressed on mobile axes. **seq_F**: sequence of elementary rotations computed about fixed axes. **seq_M**: sequence of elementary rotations computed about mobile axes.

flexion/extension component, abduction/adduction component and internal/external rotation component.

As far as sensitivity to noise is concerned, the results obtained on 50 trials (parameter values selected at random in the predefined intervals) are summarised in Table 1. The errors are expressed as a percentage of the corresponding parameter mean amplitudes.

The sensitivity of the various methods essentially differs in the internal/external rotation component, for which the result best fitting the reference values (mean error $\approx 3\%$, max. error $\approx 6\%$) is obtained using the components of the attitude vector expressed in the reference frame of the body segment adjacent to the joint. Note that the results obtained using a sequence of elementary rotations about mobile axes, corresponding to the convention proposed by Grood and Suntay (1983), are rather equivalent. This last remark is true for the knee joint, because the rotation amplitude about the floating axis is very small (Woltring, 1994), but the results for the same sequence would be worse for other joints if the adjacent segments pass through a singular attitude during the studied motion. The worst results are obtained

Table 1
Sensitivity of the four expressions to measurement noise: mean and (maximum) errors

	Flexion/Extension		Abduction/Adduction		Int. / Ext. Rotation	
	Fixed axes	Mob. axes	Fixed axes	Mob. axes	Fixed axes	Mob. axes
Rot. vector	0.5% (0.7%)	0.5% (0.7%)	6.0% (7.6%)	5.5% (7.1%)	2.9% (6.3%)	5.1% (10.1%)
Sequence	0.5% (0.6%)	0.4% (0.6%)	5.9% (7.5%)	5.5% (7.4%)	14.2% (28.3%)	3.8% (8.8%)

using a sequence about fixed axes embedded in the thigh body segment (mean error ≈ 14%, max. error ≈ 28%).

Further, from a clinical interpretation viewpoint, the time variations obtained for knee abduction/adduction and internal/external rotation using both the attitude vector projected on fixed axes and the elementary rotations about mobile axes are consistent with the anatomy: the external rotation angle is well coupled with the flexion value and the abduction/adduction component remains small.

4. Conclusion

This study compares distinct possible expressions of 3D joint kinematics, especially from the viewpoint of the sensitivity to measurement noise. This work highlights that the comparison is difficult, because many concepts and expressions are used, leading to results which cannot be compared from one study to another. A standardisation of the kinematics calculation is needed to complete that of the reference frames proposed by the CAMARC II European project (Cappozzo et al., 1995).

In this paper, two concepts have been tested: the spatial attitude vector, and a sequence of elementary rotations about successive axes. For both methods, two sets of axes have been chosen. The first one deals with the anatomical frame embedded in the proximal segment (fixed axes). The second one is formed by one axis belonging to the proximal segment, one axis belonging to the distal segment and a floating axis defined as the cross-product between the two previous ones (mobile axes).

The concept of the spatial attitude vector is obviously the only one that allows a standardisation for all joints, since the calculations are not perturbed by the "gimbal-lock" phenomenon, leading to choose distinct sequence orders adapted to each joint. Further, the criterion of the sensitivity to marker trajectory perturbations shows (at least as far as the internal/external rotation is concerned), the advantage of using the attitude vector components expressed about axes embedded in the adjacent body segment.

References

Andriacchi, T.P., 1987. Clinical applications of the SELSPOT system, Proceedings of the Biomechanics Symposium, ASME, 84, pp. 339-342.

Blankevoort, L., Huiskes, R., De Lange, A., 1990. Helical axes of passive knee joint motions. Journal of Biomechanics 23 (12), 1219–1229.

Cappello, A., Cappozzo, A., La Palombara, P.F., Lucchetti, L., Leardini, A., 1997. Multiple anatomical landmark calibration for optimal bone pose estimation. Human Movement Science 16 (2–3), 259–274.

Cappozzo, A., Catani, F., Della Croce, U., Leardini, A., 1995. Position and orientation in space of bones during movement: anatomical frame definition and determination. Clinical Biomechanics 10, 171–178.

Chao, E.Y., 1980. Justification of triaxial goniometer for the measurement of human body movements. Journal of Biomechanics 13, 989–1006.

Chèze, L., Fregly, B.J., Dimnet, J., 1995a. A solidification procedure to facilitate kinematic analyses based on video system data. Journal of Biomechanics 28 (7), 879–884.

Chèze, L., Fioretti, S., 1995b. Effects of pre-processing techniques on the kinematic descriptors of lower limb joint motion. XIII International Symposium on Biotelemetry, Williamsburg, VA.

Chèze, L., Fregly, B.J., Dimnet, J., 1998. Determination of joint functional axes from noisy marker data using the finite helical axis. Human Movement Science 17, 1–15.

Chèze, L., 1998. Influence of the calculation methods and the measurement errors on joint rotations. Proceedings of the XIth Conference of the European Society of Biomechanics, in Journal of Biomechanics 31, Suppl. 1, p.149.

Dimnet, J., Guingand, M., 1984. The finite displacement vector's method: an application to the scoliotic spine. Journal of Biomechanics 17, 397–408.

Fioretti, S., Jetto, L., 1989. Accurate derivative estimation from noisy data: a state-space approach. International Journal of Systems Science 20 (1), 33–53.

Grood, E.S., Suntay, W.J., 1983. A joint coordinate system for the clinical description of three dimensional motions: Application to the knee. Journal of Biomechanical Engineering Trans. ASME 105, 136–144.

Lafortune, M., Cavanagh, P., Sommer, H.J., Kalenak, A., 1992. 3D kinematics of the human knee during walking. Journal of Biomechanics 25, 347–357.

Lucchetti, L., Cappozzo, A., Cappello, A., Della Croce, U., 1998. Skin movement artefact assessment and compensation in the estimation of knee-joint kinematics. Journal of Biomechanics 31 (11), 977–984.

Mann, R.W., Antonsson, E.K., 1983. Gait analysis: Precise, rapid, automatic 3D position and orientation. kinematics and dynamics. Bulletin of the Hospital for Joint Diseases. Orthopaedic Institute. XLIII (2), 137–146.

Skalli, W., Lavaste, F., Descrimes, J.L., 1995. Quantification of 3D vertebral rotations in scoliosis: what are the true values? Spine 20(5), 546–553.

Söderkvist, I., Wedin, P.A., 1993. Determining the movements of the skeleton using well-configured markers. Journal of Biomechanics 26 (12), 1473–1477.

Spoor, C.W., Veldpaus, F.E., 1980. Rigid-body motion calculated from spatial co-ordinates of markers. Journal of Biomechanics 13, 391–393.

Spoor, C.W., 1984. Explanation, verification and application of helical axis error propagation formulas. Human Movement Science 3, 95–117.

Veldpaus, F.E., Woltring, H.J., Dortmans, L.J.M.G., 1988. A least-squares algorithm for the equiform transformation from spatial marker coordinates. Journal of Biomechanics 21, 45–54.

Woltring, H.J., Huiskes, R., De Lange, A., 1983. Measurement error influence on helical axis accuracy in the description of 3D finite joint movement in biomechanics. Proceedings of the Biomechanics Symposium. ASME, New York, USA, pp. 19–22.

Woltring, H.J., Huiskes, R., De Lange, A., Veldpaus, F., 1985. Finite centroid and helical axis estimation from noisy landmark measurements in the study of human joint kinematics. Journal of Biomechanics 18, 379–389.

Woltring, H.J., 1994. 3D attitude representation of human joints: a standardization proposal. Journal of Biomechanics 27 (12), 1399–1414.